Magnetoresistance behavior of ferromagnetic shape memory alloy $Ni_{1.75}Mn_{1.25}Ga$

S. Banik,[1] R. Rawat,[1] P. K. Mukhopadhyay,[2] B. L. Ahuja,[3] Aparna Chakrabarti,[4] P. L. Paulose,[5] Sanjay Singh,[1] Akhilesh Kumar Singh,[6] D. Pandey,[6] and S. R. Barman[1,*]

[1]*UGC-DAE Consortium for Scientific Research, Khandwa Road, Indore 452017, India*

[2]*LCMP, S. N. Bose National Centre for Basic Sciences, Kolkata 700098, India*

[3]*Department of Physics, M. L. Sukhadia University, Udaipur 313001, India*

[4]*Raja Ramanna Centre for Advanced Technology, Indore 452013, India*

[5]*Tata Institute of Fundamental Research, Homi Bhabha Road, Mumbai 400005, India*

[6]*School of Materials Science and Technology, Banaras Hindu University, Varanasi 221005, India*

(Received 10 December 2007; revised manuscript received 11 February 2008; published 11 June 2008)

A negative-positive-negative switching behavior of magnetoresistance (MR) with temperature is observed in a ferromagnetic shape memory alloy $Ni_{1.75}Mn_{1.25}Ga$. In the austenitic phase between 300 and 120 K, MR is negative due to *s-d* scattering. Curiously, below 120 K MR is positive, while at still lower temperatures in the martensitic phase, MR is negative again. The positive MR cannot be explained by Lorentz contribution and is related to a magnetic transition. Evidence for this is obtained from *ab initio* density-functional theory, a decrease in magnetization and resistivity upturn at 120 K. Theory shows that a ferrimagnetic state with antiferromagnetic alignment between the local magnetic moments of the Mn atoms is the energetically favored ground state. In the martensitic phase, there are two competing factors that govern the MR behavior: a dominant negative trend up to the saturation field due to the decrease in electron scattering at twin and domain boundaries and a weaker positive trend due to the ferrimagnetic nature of the magnetic state. MR exhibits a hysteresis between heating and cooling that is related to the first-order nature of the martensitic phase transition.

DOI: 10.1103/PhysRevB.77.224417 PACS number(s): 75.50.Cc, 71.15.Nc, 81.30.Kf, 75.47.−m

I. INTRODUCTION

Recent years have witnessed extensive research on magnetoresistance (MR) to understand its basic physics in metallic multilayers, transition-metal oxides, etc.[1] Ferromagnetic shape memory alloys (FSMAs) are of current interest because of their potential technological applications and the rich physics they exhibit.[2–12] Large magnetic-field induced strain (MFIS) of 10% with actuation that is faster than conventional shape memory alloys (SMAs) has been obtained in Ni-Mn-Ga.[13,14] MFIS is achieved by twin boundary (TB) rearrangement in the martensitic phase and the main driving force for TB motion in the presence of a magnetic field is the large magnetocrystalline anisotropy (MCA).[13–19]

Negative MR has been observed earlier in SMAs such as Cu-Mn-Al and was associated with the possible presence of Mn-rich clusters in the Cu_2AlMn structure.[20] Recently, we have reported a negative MR of about 7.3% at 8 T at room temperature (RT) in $Ni_{2+x}Mn_{1-x}Ga$.[21] It was explained by *s-d* scattering model for a ferromagnet, while the differences in the MR behavior in the martensitic phase compared to the austenitic phase were related to twin variant rearrangement with magnetic field.[21] MR ranging between −1% and −4.5% has been reported for thin films of Ni-Mn-Ga.[22,23] Recently, a large negative MR of 60%–70% has been reported for Ni-Mn-In, which has been explained by the shift of the martensitic transition temperature with magnetic field.[24,25]

$Ni_{2-y}Mn_{1+y}Ga$ with $y=0.25$, i.e., $Ni_{1.75}Mn_{1.25}Ga$, is one of the unique compositions in the Ni-Mn-Ga family that has low martensitic transition temperature (M_s) of about 76 K.[26] This enables the study of the ferroelastic transition much below the Curie temperature ($T_C=380$ K). Here, part of the Mn atoms ($y=0.25$), referred to as Mn I, occupy the Ni site, while the remaining Mn ($y=1.0$) atoms at the Mn site are referred to Mn II. The Mn I atoms, which are 20% of the total Mn atoms, are excess with respect to the stoichiometric Ni_2MnGa composition. These excess Mn I-type atoms are expected to have interesting influence on the resistivity, MR, and magnetization, since in related systems such as $Ni_2Mn_{1.25}Ga_{0.75}$ and Mn_2NiGa their moments are reported to be antiparallel to the Mn II atoms.[10,27] Here, we report an intriguing switching behavior of MR with temperature that is related to the occurrence of martensitic transition at low temperature in the ferrimagnetic state. To the best of our knowledge, such MR behavior reported here has not been observed in any magnetic material up to date. This basically arises from the interplay of magnetism and shape memory effect. Our studies indicate possibility of practical applications for ferromagnetic SMA as magnetic sensor for data storage and encryption, whose response can be toggled by changing the temperature. It is envisaged that the multifunctional combination of properties (magnetic sensing, magnetocaloric, actuation, and shape memory effects) of the ferromagnetic SMAs will be important for their future application.

II. METHODS

Bulk polycrystalline ingots of $Ni_{1.75}Mn_{1.25}Ga$ have been prepared by the standard method of melting appropriate quantities of Ni, Mn, and Ga (99.99% purity) in an arc furnace. The ingot was annealed at 1100 K for nine days for homogenization and subsequently quenched in ice water.[12,28] The composition has been determined by energy dispersive analysis of x rays using a JEOL JSM 5600 electron micro-

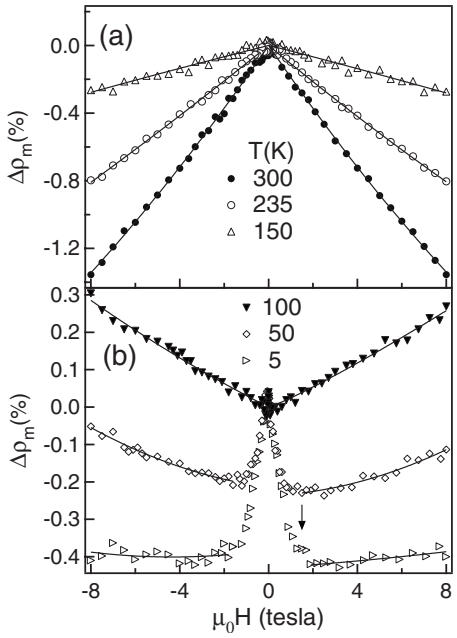

FIG. 1. Isothermal magnetoresistance (MR=$\Delta\rho_m$) of $Ni_{1.75}Mn_{1.25}Ga$ as a function of magnetic field at different temperatures [(a) 300–150 K and (b) 100–5 K]. MR has been measured in the cooling cycle. The arrow indicates the saturation magnetic field at 20 K. The solid lines are fit to the data.

scope. A superconducting magnet from Oxford Instruments, Inc., U.K. was used for carrying out the longitudinal MR measurements up to a maximum magnetic field of 8 T.[29] MR is defined as $\Delta\rho_m=\frac{\Delta\rho}{\rho_0}=\frac{(\rho_H-\rho_0)}{\rho_0}$, where ρ_H and ρ_0 are the resistivities in H and zero field, respectively. The statistical scatter of the resistivity data is 0.03%. $M(T)$ measurements were performed with Lakeshore 7404 vibrating sample magnetometer with a close cycle refrigerator. $M(H)$ measurements were done using a MPMS XL5 superconducting quantum interference device (SQUID) magnetometer. Temperature-dependent powder x-ray diffraction (XRD) data were collected using an 18 kW copper rotating anode-based Rigaku powder diffractometer fitted with a graphite monochromator in the diffracted beam. The temperature was stable within ± 0.3 K during data collection at each temperature. The data were collected in the Bragg–Brentano geometry using a scintillation counter.

Spin-polarized first-principles density-functional theory calculations were performed by full potential linearized augmented plane-wave (FPLAPW) method using the WIEN97 code.[30] Generalized gradient approximation for the exchange correlation was used.[31] The muffin-tin radii were taken to be 2.1364 a.u. for Ni, 2.2799 a.u. for Mn, and 2.1364 a.u. for Ga. The convergence criterion for total energy was 0.1 mRy, i.e., an accuracy of ± 0.34 meV/atom. The details of the method of calculation are given elsewhere.[9,10]

III. RESULTS AND DISCUSSION

Figure 1 shows the isothermal magnetoresistance ($\Delta\rho_m$) of $Ni_{1.75}Mn_{1.25}Ga$ as a function of magnetic field at different temperatures. It can been seen from the figure that at 300 K, the magnitude of $\Delta\rho_m(H)$ increases with H to −1.35% at 8 T [Fig. 1(a)]. In order to ascertain the H dependence, we have fitted $\Delta\rho_m(H)$ by a second-order polynomial of the form $\alpha H+\beta H^2$ (solid lines in Fig. 1). We find the second-order term (β) to be very small, and the ratio β/α being 0.02, which shows that the variation is essentially linear. Similar linear variation is obtained down to 150 K, although the magnitude of $\Delta\rho_m$ decreases to −0.3%. Linear variation of negative MR with field has been observed for Ni_2MnGa.[21] Also Kataoka[32] calculated $\Delta\rho_m(H)$ for ferromagnets with different electron concentrations using the *s-d* scattering model, where the scattering of *s* conduction electrons by localized *d* spins is suppressed by the magnetic field resulting in a decrease in ρ. Magnitude of $\Delta\rho_m$ is shown to increase almost linearly with H for ferromagnetic materials.[32] Since $Ni_{1.75}Mn_{1.25}Ga$ has large Mn $3d$ local moment with high electron concentration (valence electron to atom ratio, e/a =7.31), negative MR in the 150–300 K range is well described by the *s-d* scattering model. As the temperature is lowered, $\Delta\rho_m(H)$ decreases due to reduction in the spin disorder scattering.

MR in Fig. 1(b) shows an interesting behavior: $\Delta\rho_m(H)$ is positive at 100 K. However, at 50 K it is negative but with a different H dependence compared to the *s-d* scattering regime [Fig. 1(a)]. In other ferromagnetic Heusler alloys, such as Ni_2MnSn and Pd_2MnSn, positive MR has been observed and attributed to the Lorentz contribution.[33] In such cases, $\Delta\rho_m$ is positive at lowest temperatures and decreases as temperature increases. For example, MR is positive for Pd_2MnSn at 1.8 K and is negative above 60 K.[33] In contrast, the MR variation in $Ni_{1.75}Mn_{1.25}Ga$ is opposite. Lorentz contribution gives rise to a positive MR when the condition $\omega_C\tau \gg 1$ is satisfied, where ω_C and τ are cyclotron frequency and conduction-electron relaxation time, respectively. This condition is valid for extremely pure metallic single crystals at very low temperatures (where τ is large and $\rho \leq 10^{-8}$ Ω cm) or at large H (where ω_C is large). However, for $Ni_{1.75}Mn_{1.25}Ga$, the residual resistivity is large, implying small τ so that even at 8 T the above condition is not satisfied. By the same argument, we expect a more positive contribution at 5 K compared to 50 K, since the resistivity is lower at 5 K [Fig. 2(a)]. On the other hand, the observed data show opposite trend. Hence, the positive MR in $Ni_{1.75}Mn_{1.25}Ga$ cannot be ascribed to Lorentz force and other mechanisms need to be explored to understand this finding.

Figure 2(a) shows resistivity [$\rho(T)$] at 0 and 5 T magnetic field between 5 and 180 K for two cycles. Above 120 K, where the sample is in the austenitic phase, $\rho(T)$ has a positive temperature coefficient of resistance, and the data for the different cycles overlap. Between 88 and 37 K, the hysteresis in $\rho(T)$ becomes highly pronounced and this is a signature of the martensitic transition. The martensitic transition is also clearly shown by the ac-susceptibility data in Ref. 26 and the low-field magnetization data shown in Fig. 4(a) (discussed latter). The onset of the martensitic transition is depicted by the change in slope in ρ at M_s (=76 K, in agreement with Ref. 26). The other transition temperatures such as martensite finish M_f=37 K, austenitic start A_s=47 K, and austenitic finish A_f=88 K, shown in Fig. 2(a), concur with the

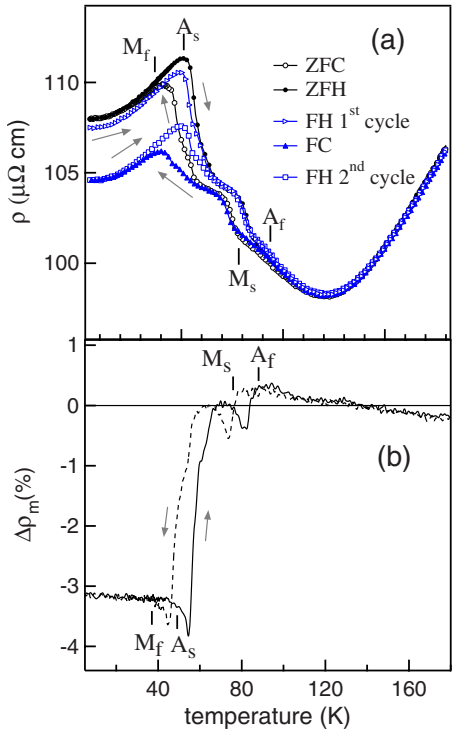

FIG. 2. (Color online) (a) Resistivity (ρ) as a function of temperature at 0 and 5 T field for $Ni_{1.75}Mn_{1.25}Ga$ between 5 and 180 K for two cooling and heating cycles. The data have been recorded in the following sequence: zero-field heating (ZFH), zero-field cooling (ZFC), the sample is then subjected to a magnetic field of 5 T, and field-cooled heating (FH, first cycle) is done up to RT, field-cooled (FC) cooling, and once again FH (second cycle) was measured. A_s, A_f, M_s, and M_f are the austenitic and martensitic start and finish temperatures, respectively. (b) Magnetoresistance during cooling and heating calculated from the difference of $\rho(T)$ at 0 and 5 T after interpolating to same temperature intervals. The difference has been taken between ZFC and FC in the cooling cycle and ZFH and FH second cycle while heating.

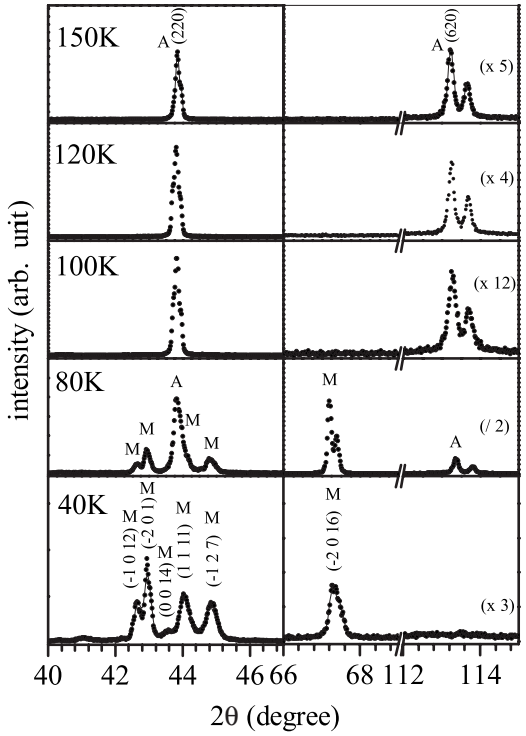

FIG. 3. X-ray diffraction pattern of $Ni_{1.75}Mn_{1.25}Ga$ as a function of temperature while cooling. The calculated profiles obtained by Le Bail fitting (solid line through the experimental data points) are shown for 150 and 40 K data. *A* and *M* indicate the peaks related to the austenitic and martensitic phases, respectively.

$M(T)$ data to be discussed later [Fig. 4(a)]. ρ shows a step centered around 65 K. This possibly arises due to strain effect on the nucleation and growth of the martensitic phase at such low temperatures, and similar effect has been observed in Ni_2FeGa.[26]

In order to establish beyond any doubt that the hysteresis in $\rho(T)$ is related to the martensitic transition, we show the powder XRD pattern at different temperatures in Fig. 3. To record the XRD patterns, $Ni_{1.75}Mn_{1.25}Ga$ ingot was crushed to powder and annealed at 773 K for 10 h to remove the residual stress. The L_{2_1} cubic austenitic phase is observed up to 100 K. There is no signature of any phase transition, related to the formation of a possible premartensitic phase around 120 K, which could have been responsible for the upturn in $\rho(T)$. The lattice constant at 100 K turns out to be $a_{aus}=5.83$ Å. At 80 K, extra peaks corresponding to the martensitic phase appear and these coexist with the austenitic peaks. By 40 K, the XRD pattern shows that the martensitic transition is complete as there is no austenite phase, in agreement with the $\rho(T)$ data. The XRD patterns have been indexed by Le Bail fitting procedure,[34] and we find that the martensitic phase is monoclinic in the $P2/m$ space group. The refined lattice constants are $a=4.22$, $b=5.50$, $c=29.18$ Å, and $\beta=91.13$. Since $c\approx 7a$, a seven layer modulation may be expected, and such modulated structures with monoclinic or orthorhombic symmetry have been reported for Ni-Mn-Ga.[35] Magnetic field induced strain has been observed in Ni-Mn-Ga for structures that exhibit modulation.[13,14] The unit-cell volume of the martensitic phase is within 2% of that of the equivalent austenitic cell given by $7a_{aus}^3/2$. This shows that the unit-cell volume changes little between the two phases, as expected for a shape memory alloy.[36]

After establishing the existence of the structural martensitic transition from XRD, we discuss the details of the resistivity behavior. $\rho(T)$ at 5 T shows a difference in the first and second field heating (FH) cycles, the first cycle $\rho(T)$ being higher. In the first FH cycle, the sample is subjected to a magnetic field of 5 T at 5 K after zero-field cooling (ZFC). Subsequently, field cooled (FC) data were taken and then the second cycle of FH was measured. Thus, while in FH first cycle, the magnetic field of 5 T was switched on at 5 K, where as in the FH second cycle the field is on from RT. The possible reason for the difference in resistivity between the two FH cycles will be discussed later on. In Fig. 2(b), we show the MR calculated from the difference between the ZFC and FC (cooling MR data) and zero-field heating (ZFH) and FH second cycle (heating MR data). However, if the FH first cycle is considered, MR is lower by about 0.4% at 5 K, which agrees with the value in Fig. 1. This is because the

MR in Fig. 1 is measured in a different way: at 300 K, H is varied from 0 to 8 to 0 to −8 to 0 T. Then, the specimen was cooled down to the next measurement temperature of 235 K and the field was varied in a similar way. For the next measurement, the sample was heated up to 300 K and cooled under zero-field condition to the temperature of measurement. Thus, for the martensitic phase, this MR data (Fig. 1) can be related to $\Delta\rho_m$ calculated from ZFH and FH first cycle ρ data [Fig. 2(a)].

Figure 2(b) clearly shows the switching effect in MR as a function of temperature. A comparison of Figs. 2(a) and 2(b) shows a significant correlation between the hysteresis in MR and $\rho(T)$. For the cooling cycle, MR is negative from 300 to 135 K and exhibits a negative to positive switching at 135 K. This negative MR region is explained by s-d scattering, as discussed above. MR is positive between 135 and 76 K ($=M_s$), and this is also manifested in MR(H) data at 100 K in Fig. 1(b). As discussed earlier, the positive MR cannot be assigned to Lorentz force contribution. MR exhibits a positive to negative switching at M_s in the cooling cycle. MR becomes negative at M_s with a shallow minimum at 73 K, shows a hump at 64 K, then plunges to large negative values below 64 K, and finally increases slightly to reach a temperature independent value of about −3% below 37 K ($=M_f$). The shape of the MR(T) curve in Fig. 2(b) during heating is very similar to that during cooling but is shifted in temperature in the martensitic transition region due to hysteresis. Thus, hysteresis in MR is clearly observed, which indicates the possibility of studying phase coexistence and first-order phase transition in FSMAs using MR.

Magnetization measurements have been performed to understand the magnetoresistance behavior. A sharp decrease in magnetization at the martensitic transition [Fig. 4(a)] in small fields (0.01–0.1 T) is the manifestation of large MCA in the martensitic phase.[37] Large MCA has been observed in different Ni-Mn-Ga alloys and is responsible for magnetic field induced twin variant reorientation. The magnetization in the martensitic phase decreases because in the low field, a twinned state with moments along the easy axis ([001]) oriented in dissimilar directions for different twins is energetically favorable. The gradual decrease in magnetization in the austenitic phase, on the other hand, is possibly related to an increase in the austenitic phase MCA with decreasing temperature.[37] A steplike decrease in magnetization with distinct change of slope is evident at 120 K for both 0.01 and 0.1 T fields [inset of Fig. 4(a)]. This decrease is significant because it suggests that the upturn in $\rho(T)$ and positive MR could be related to a magnetic transition that decreases the magnetization.

Figure 4(b) shows $M(T)$ at 5 T in FC and FH. This field is much higher than the saturation field, as shown by the isothermal M-H curves in Fig. 5. $M(T)$ shows the characteristic variation of saturation magnetization with temperature. By fitting the higher temperature region using the expression $(T_C-T)^{\gamma}$ [bold dashed line in Fig. 4(b)], we obtain an approximate estimate of T_C to be 380 K. This is close to the T_C of 385 K reported for $Ni_{1.8}Mn_{1.2}Ga$.[26] In comparison to Fig. 4(a), magnetization increases by 2 orders of magnitude for 5 T FC and FH runs. Thus, the changes in the magnetization that are clearly visible in the low-field measurement [Fig. 4(a)] are not evident here. For example, the large relative decrease in magnetization in the martensitic phase [Fig. 4(a)] and the decrease at 120 K are not observed in Fig. 4(b). Instead, the magnetization gradually increases in the martensitic phase. This increase is intrinsic and is due to higher saturation magnetization in the martensitic phase. This results from alterations in interatomic bonding related to the change of structure, as also observed in Ni_2MnGa.[8,38] The saturation moment turns out to be $3.5\mu_B$. The only signature of the martensitic transition in Fig. 4(b) is the hysteresis in $M(T)$ during heating and cooling cycles. However, there is

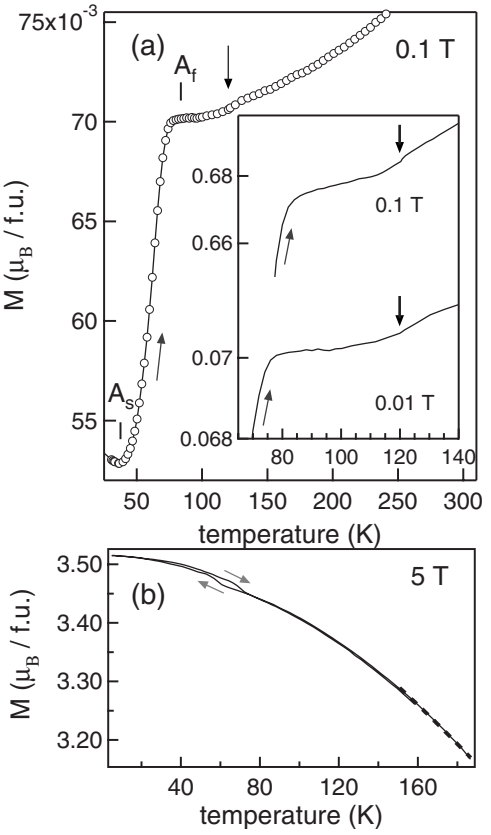

FIG. 4. Temperature dependence of magnetization in (a) a small applied field of 0.01 T during heating after zero-field cooling; the inset shows the expanded region around 120 K for two different fields (0.01 and 0.1 T); (b) high field of 5 T during FC and FH. The dashed line is a fit to the data (see text).

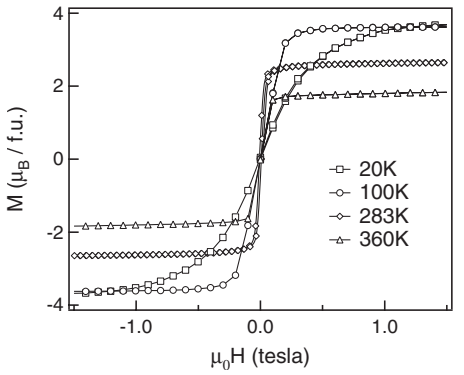

FIG. 5. Isothermal M-H loops at different temperatures.

hardly any change in the M_s with field. This shows that for this alloy, magnetic field does not change M_s resulting in magnetic field induced martensitic transition, unlike in Ni-Mn-Sn and Ni-Mn-In.[3] The isothermal M-H loop in Fig. 5 shows a decrease in the saturation magnetic field between the martensitic phase (20 K) and the austenitic phase (283 or 360 K). This is because in the austenitic phase, the MCA is very small and there is no twinning compared to the martensitic phase with large MCA and twinning.

We have calculated the magnetic ground state using *ab initio*, spin polarized density-functional theory employing FPLAPW method to understand the origin of positive MR behavior. Good agreement between experiment and theory has been obtained earlier for the magnetic moments, the lattice constants, the total energies, and the density of states for both the phases.[8–10,12,28] In particular, the total energies have been used to explain the phase diagram and magnetic states of Ni_2MnGa, $Ni_{2.25}Mn_{1.75}Ga$, and Mn_2NiGa.[9,10]

Here, we calculate the total energies of the different magnetic states of nonstoichiometric $Ni_{1.75}Mn_{1.25}Ga$ for the $L2_1$ structure (see Fig. 1 in Ref. 8) with lattice constant of 5.843 Å determined from XRD at room temperature. The structure consists of four interpenetrating fcc sublattices occupied by two Ni atoms, one Mn (Mn II), and one Ga atom. To emulate the nonstoichiometric composition, a 16 atom $L2_1$ supercell is considered, where one of the eight Ni atoms is replaced by one excess Mn I-type atom.[9] Thus, there are seven Ni, five Mn (one Mn I and four Mn II, i.e., out of total Mn atoms only 20% are Mn I), and four Ga atoms in the supercell with the chemical formula $Ni_7Mn_5Ga_4$, which is equivalent to $Ni_{1.75}Mn_{1.25}Ga$. The total energy that consists of the total kinetic, potential, and exchange-correlation energies of a periodic solid with frozen nuclei has been calculated for two magnetic configurations with Mn I spin moment parallel and antiparallel to Mn II. We find that the total energy is significantly lower by 16 meV/atom, when Mn I is antiparallel to Mn II, compared to their parallel orientation. Antiparallel alignment of Mn spins is energetically favored because of the direct Mn I-Mn II nearest-neighbor (at 2.53 Å distance) interaction, as has been shown for other Mn excess systems such as Mn_2NiGa, $Ni_2Mn_{1.25}Ga_{0.75}$, and Ni-Mn-Sn.[3,10,27] The exchange pair interaction as a function of Mn-Mn separation was calculated by a Heisenberg-type model and an antiferromagnetic coupling at short interatomic distances was found.[39] Enkovaara *et al.*[27] reported antiferromagnetic Mn configuration in $Ni_2Mn_{1.25}Ga_{0.75}$ from magnetization and first-principles calculations. Here for $Ni_{1.75}Mn_{1.25}Ga$, the Ni magnetic moment ($0.3\mu_B$) is parallel to Mn II. The Mn I and Mn II moments for the antiparallel (parallel) orientation are unequal: $-2.74\mu_B$ ($1.9\mu_B$) and $3.23\mu_B$ ($3.16\mu_B$), respectively. Thus, the magnetic moment of Mn I is smaller than Mn II. Smaller magnetic moment for Mn I has also been obtained for Mn_2NiGa, and this has been assigned to stronger hybridization between the majority-spin Ni and Mn II $3d$ states in comparison to hybridization between Ni and MnI Mn I $3d$ minority-spin states.[10]

The difference in total energy between the paramagnetic and ferromagnetic phases of Ni_2MnGa was equated to k_BT_C.[40] Following a similar approach, the total-energy difference between the ferromagnetic and ferrimagnetic states (16 meV/atom) corresponds to 186 K. As discussed earlier, $M(T)$ shows a decrease in magnetization at 120 K, which is indicative of a magnetic transition. Since from theory, we find that the Mn I atoms have magnetic moment different from and antiparallel to the Mn II atom, we term the state below 120 K to be ferrimagnetic. Here, antiparallel alignment of unequal local Mn moments would exist for those Mn II atoms that have Mn I as a nearest neighbor. The estimate of a transition temperature of 186 K from theory can be considered to be in fair agreement with the experiment (120 K), considering that theory considers an ideal situation while the actual conditions may be more complicated. For example, the Mn I atoms would replace the Ni atoms at random positions, and the absence of any superlattice peak in the XRD pattern (Fig. 3) indeed indicates that. This disorder effect is not considered in theory. Moreover, antisite defects, possibility of canted alignment, are not considered by theory. So, in reality, the lattice sites where antiparallel alignment between Mn I and Mn II moments occurs would be random and the moment of Mn I could be less than what is calculated. In fact, this is indicated by the underestimation of the total moment by theory ($3.1\mu_B$) compared to the experimental value of $3.5\mu_B$ [Fig. 4(b)].

To explain the positive MR shown in Figs. 1 and 2, we note that the application of magnetic field to a state with partial antiferromagnetic alignment of moments (Mn I and Mn II in this case) would induce spin fluctuations, thus increasing the spin disorder and hence resistivity that would result in positive MR.[41,42] In $Eu_{0.83}Fe_4Sb_{12}$, large positive MR has been assigned to a ferrimagnetic or canted magnetic phase.[41] We also find that for $Ni_{1.75}Mn_{1.25}Ga$, positive MR increases linearly with field. In many antiferromagnetic intermetallic alloys, positive MR has been observed to increase linearly with H.[43] For $Eu_{0.83}Fe_4Sb_{12}$, at low temperatures a $H^{2/3}$ variation was observed. Linear positive MR has been recently reported for Fe, Co, and Ni thin films up to 60 T and has been explained by quantum electron-electron interaction theory.[44] To the best of our knowledge, no theoretical prediction exists about MR behavior for a ferrimagnet with disordered antiferromagnetic alignment of a fraction of the local moments. To understand the linear MR variation in $Ni_{1.75}Mn_{1.25}Ga$, measurements with higher fields would constitute an interesting study.

In the martensitic phase, MR is negative and its magnitude increases up to the saturation field [5 and 50 K data in Fig. 1(b)]. However, the behavior is clearly different from the austenitic phase: the slope of MR(H) does not change with temperature between 0 and 2 T [see the 5 and 50 K plots in Fig. 1(b)]. In contrast, the slope changes between 300, 235, and 150 K data in the austenitic phase where s-d scattering dominates. This indicates that the origin of negative MR is different in the martensitic phase. Unlike in Ni_2MnGa,[21] here the T_C (=380 K) is much higher than M_s (=76 K) and so the effect of s-d scattering in the martensitic phase is not visible.

One of the reasons for the increase in ρ in the martensitic phase is the scattering of the Bloch wave functions at the TBs, which are known to increase the defect density and hence resistivity;[45] and this has been reported earlier for FSMAs.[46,47] The origin of negative MR in the martensitic

phase that leads to positive to negative switching of MR while cooling [Figs. 1(b) and 2(b)] possibly arises from the decrease in electron scattering due to decrease in the density of TBs and domain walls with the application of external magnetic field. These are oriented in dissimilar directions at zero field and would tend to form larger twin variants and domains as the saturation field is reached. This will have smaller resistivity compared to the twinned state with small sized twins and domains at $H=0$.[19,48] Negative MR due to domain-wall scattering has been observed in ferromagnetic thin films.[49–52] The hysteresis normally observed in domain-wall MR is related to the hysteresis of the M-H curve. However, for $Ni_{1.75}Mn_{1.25}Ga$ the M-H curves hardly exhibit any hysteresis (Fig. 5). For $Ni_{1.75}Mn_{1.25}Ga$, the observation that the increase in the negative MR magnitude occurs for fields less than equal to the saturation field [arrow, Fig. 1(b)] suggests that its origin is linked with the twin and domain rearrangement.

TB motion occurs when twinning stress is small and MCA is high governed by the condition $K > \epsilon_0 \sigma_{tw}$, where K is the magnetic anisotropy energy density, σ_{tw} is the twinning stress, and ϵ_0 is the maximal strain given by $(1-c/a)$.[14] For this specimen, high MCA is expected because M_s is much lower than T_C and this is supported by magnetization data in Fig. 4(a). In fact, the decrease in magnetization at M_s gives rise to inverse magnetocaloric effect, and its magnetic-field dependence has been explained by twin variant reorientation.[53] From XRD, we find that the unit-cell volume remains similar across the martensitic transition and the structure is modulated in the martensitic phase (Fig. 3). Modulated structures have lower twinning stress and hence are expected to exhibit TB motion.[54] These indicate that $Ni_{1.75}Mn_{1.25}Ga$ would have small twinning stress and thus exhibit TB motion. In fact, highest MFIS of 10% has been reported in a Mn excess specimen with composition of $Ni_{1.95}Mn_{1.19}Ga_{0.86}$ that exhibits seven layer modulated structure and a low twinning stress of 2 MPa.[14] MFIS has been reported to occur in polycrystals that are textured and with large grain size in trained samples and also in fine grained systems.[6,16,18,55–57] In our case, the specimen has been annealed for more than a week at 1100 K, and that leads to the growth of large grains (200–500 μm). On the other hand, in the absence of field, the width of the twins is only a few microns.[19,48,58] Thus, within a grain the twins are ubiquitous and TB rearrangement can occur due to external magnetic field. Coarse grained Ni-Mn-Ga is known to show larger MFIS, while annealing of Ni-Mn-Ga ribbons is reported to increase the MFIS by an order of magnitude.[59] Sozinov *et al.*[18] obtained single variant state for polycrystalline Ni-Mn-Ga at 1 T. For polycrystals, since the grains are oriented randomly, which lead to internal geometric constraints, for example, the motion of the twin boundaries would be suppressed by the grain boundaries, the macroscopic strain is small. However, at the microscopic level within a grain, the TB motion is expected to occur in $Ni_{1.75}Mn_{1.25}Ga$ and this is what is important in the present context to explain the negative MR behavior in the martensitic phase. The shape of the MR(H) curve in the martensitic phase in polycrystalline Ni-Mn-Ga has been explained by twin variant rearrangement with magnetic field.[21]

The difference in resistivity between the first and second FH cycles (Fig. 2) can be related to the extent of TB rearrangement. Lower values of $\rho(T)$ in second FH cycle, which is recorded after cooling in the presence of magnetic field across the martensitic transition from 300 K, indicate that the field would more effectively reorient the twins as soon as these are formed below M_s. On the other hand, for FH first cycle where ρ is higher the magnetic field is switched on at 5 K. Thus, although MCA increases with decreasing temperature,[37] twinning stress may also increase limiting the extent of twin variant rearrangement forming larger twins. The variation of negative MR with temperature in the martensitic phase shown in Fig. 2(b) is significant because the heating and cooling data are very similar. This may be related to the microscopic details of the domain and twin variant reorientation with temperature and further studies are required to explain this.

Another interesting observation in the MR of the martensitic phase is as follows: above the saturation field although MR is negative, a positive component is evident from its gradual increase with field [see Fig. 1(b)]. For example, at 50 K MR increases from −0.2% at 1 T to −0.1% at 8 T. A weakly increasing MR is also observed for the 5 K data, but its slope is less compared to 50 K. This shows that at lower temperatures where thermal fluctuations decrease, higher field would be required to induce spin disorder in the ferrimagnetic state for causing similar increase in MR. This, in turn, supports the argument that below 120 K the magnetic state is ferrimagnetic in nature. Thus, there are two competing effects that govern MR in the martensitic phase with increasing field: a dominant negative trend due to the formation of larger size twin variants and domains and a weaker positive trend due to the ferrimagnetic nature of the magnetic state. While the first effect is present only up to the saturation field, the second effect becomes visible only above the saturation field.

IV. CONCLUSION

The switching of MR from negative to positive and back to negative values with decreasing temperature is observed in a Mn excess ferromagnetic shape memory alloy $Ni_{1.75}Mn_{1.25}Ga$. Positive MR below 120 K in the austenitic phase is related to a ferrimagnetic state where the excess Mn atoms (Mn I) at Ni site are antiferromagnetically oriented with the Mn atoms at Mn site (Mn II). The existence of the ferrimagnetic state is shown by density-functional theory, and experimental evidence is obtained from a decrease in magnetization and resistivity upturn at 120 K. In the martensitic phase, negative MR arises due to decrease in electron scattering related to reduction in the density of TBs and domain walls with the application of external magnetic field. This effect is visible up to the saturation magnetic field. Above this, a weaker positive trend due to the ferrimagnetic nature of the magnetic state is visible. On the other hand, negative MR above 120 K in the ferromagnetic austenitic phase is explained by the s-d scattering model. The hysteresis in MR(T) is a manifestation of the first-order nature of the martensitic phase transition.

ACKNOWLEDGMENTS

We are grateful to S. N. Kaul, A. K. Majumdar, E. V. Sampathkumaran, N. Lakshmi, A. Banerjee, R. Ranjan, and K. Maiti for useful discussions and support. P. Nordblad is thanked for his valuable support during the visit of PKM to his laboratory. P. Chaddah, K. Horn, A. K. Raychaudhuri, V. C. Sahni, B. K. Sharma, A. Gupta, and S. M. Oak are thanked for constant encouragement. Research grants from Ramanna Research Grant, Max Planck partner group project, Department of Science and Technology, India, and SIDA, Sweden are acknowledged.

*barman@csr.ernet.in

[1] M. N. Baibich, J. M. Broto, A. Fert, F. Nguyen Van Dau, F. Petroff, P. Eitenne, G. Greuzet, A. Friederich, and J. Chazelas, Phys. Rev. Lett. **61**, 2472 (1988); S. Jin, T. H. Tiefel, M. McCormack, R. A. Fastnacht, R. Ramesh, and L. H. Chen, Science **264**, 413 (1994).

[2] R. Kainuma, Y. Imano, W. Ito, Y. Sutou, H. Morito, S. Okamoto, O. Kitakami, K. Oikawa, A. Fujita, T. Kanomata, and K. Ishida, Nature (London) **439**, 957 (2006).

[3] T. Krenke, E. Duman, M. Acet, E. F. Wassermann, X. Moya, L. Mañosa, and A. Planes, Nat. Mater. **4**, 450 (2005).

[4] I. Takeuchi, O. O. Famodu, J. C. Read, M. A. Aronova, K.-S. Chang, C. Craciunescu, S. E. Lofland, M. Wuttig, F. C. Wellstood, L. Knauss, and A. Orozco, Nat. Mater. **2**, 180 (2003).

[5] A. Planes, E. Obradó, A. Gonzàlez-Comas, and L. Mañosa, Phys. Rev. Lett. **79**, 3926 (1997).

[6] Y. Boonyongmaneerat, M. Chmielus, D. C. Dunand, and P. Müllner, Phys. Rev. Lett. **99**, 247201 (2007).

[7] V. A. Chernenko, V. A. L'vov, P. Müllner, G. Kostorz, and T. Takagi, Phys. Rev. B **69**, 134410 (2004).

[8] S. R. Barman, S. Banik, and A. Chakrabarti, Phys. Rev. B **72**, 184410 (2005).

[9] A. Chakrabarti, C. Biswas, S. Banik, R. S. Dhaka, A. K. Shukla, and S. R. Barman, Phys. Rev. B **72**, 073103 (2005).

[10] S. R. Barman, S. Banik, A. K. Shukla, C. Kamal, and A. Chakrabarti, Europhys. Lett. **80**, 57002 (2007); S. R. Barman and A. Chakrabarti, Phys. Rev. B **77**, 176401 (2008).

[11] B. L. Ahuja, B. K. Sharma, S. Mathur, N. L. Heda, M. Itou, A. Andrejczuk, Y. Sakurai, A. Chakrabarti, S. Banik, A. M. Awasthi, and S. R. Barman, Phys. Rev. B **75**, 134403 (2007).

[12] S. Banik, A. Chakrabarti, U. Kumar, P. K. Mukhopadhyay, A. M. Awasthi, R. Ranjan, J. Schneider, B. L. Ahuja, and S. R. Barman, Phys. Rev. B **74**, 085110 (2006).

[13] S. J. Murray, M. Marioni, S. M. Allen, R. C. O'Handley, and T. A. Lograsso, Appl. Phys. Lett. **77**, 886 (2000).

[14] A. Sozinov, A. A. Likhachev, N. Lanska, and K. Ullakko, Appl. Phys. Lett. **80**, 1746 (2002).

[15] F. Albertini, L. Morellon, P. A. Algarabel, M. R. Ibarra, L. Pareti, Z. Arnold, and G. Calestani, J. Appl. Phys. **89**, 5614 (2001).

[16] K. Ullakko, Y. Ezer, A. Sozinov, G. Kimmel, P. Yakovenko, and Y. K. Lindroos, Scr. Mater. **44**, 475 (2001).

[17] M. R. Sullivan and H. D. Chopra, Phys. Rev. B **70**, 094427 (2004).

[18] A. Sozinov, A. A. Likhachev, N. Lanska, O. Söderberg, K. Ullakko, and V. K. Lindroos, Mater. Sci. Eng., A **378**, 399 (2004).

[19] Q. Pan and R. D. James, J. Appl. Phys. **87**, 4702 (2000).

[20] J. Marcos, A. Planes, L. Mañosa, A. Labarta, and B. J. Hattink, Phys. Rev. B **66**, 054428 (2002).

[21] C. Biswas, R. Rawat, and S. R. Barman, Appl. Phys. Lett. **86**, 202508 (2005).

[22] M. S. Lund, J. W. Dong, J. Lu, X. Y. Dong, C. J. Palmstrom, and C. Leighton, Appl. Phys. Lett. **80**, 4798 (2002).

[23] V. O. Golub, A. Ya. Vovk, L. Malkinski, C. J. O'Connor, Z. Wang, and J. Tang, J. Appl. Phys. **96**, 3865 (2004).

[24] S. Y. Yu, Z. H. Liu, G. D. Liu, J. L. Chen, Z. X. Cao, G. H. Wu, B. Zhang, and X. X. Zhang, Appl. Phys. Lett. **89**, 162503 (2006).

[25] V. K. Sharma, M. K. Chattopadhyay, K. H. B. Shaeb, A. Chouhan, and S. B. Roy, Appl. Phys. Lett. **89**, 222509 (2006).

[26] G. D. Liu, J. L. Chen, Z. H. Liu, X. F. Dai, G. H. Wua, B. Zhang, and X. X. Zhang, Appl. Phys. Lett. **87**, 262504 (2005); Z. H. Liu, M. Zhang, Y. T. Cui, Y. Q. Zhou, W. H. Wang, G. H. Wu, X. X. Zhang, and G. Xiao, *ibid.* **82**, 424 (2003).

[27] J. Enkovaara, O. Heczko, A. Ayuela, and R. M. Nieminen, Phys. Rev. B **67**, 212405 (2003).

[28] S. Banik, R. Ranjan, A. Chakrabarti, S. Bhardwaj, N. P. Lalla, A. M. Awasthi, V. Sathe, D. M. Phase, P. K. Mukhopadhyay, D. Pandey, and S. R. Barman, Phys. Rev. B **75**, 104107 (2007).

[29] R. Rawat and I. Das, J. Phys.: Condens. Matter **13**, L57 (2001); A. Venimadhav, M. S. Hedge, R. Rawat, I. Das, P. L. Paulose, and E. V. Sampathkumaran, Phys. Rev. B **63**, 214404 (2001).

[30] P. Blaha, K. Schwartz, and J. Luitz, *WIEN97, A Full Potential Linearized Augmented Plane Wave Package for Calculating Crystal Properties* (Karlheinz Schwarz, Technische Universität, Austria, 1999).

[31] J. P. Perdew and K. Burke, Phys. Rev. Lett. **77**, 3865 (1996).

[32] M. Kataoka, Phys. Rev. B **63**, 134435 (2001).

[33] C. M. Hurd, I. Shiozaki, and S. P. McAlister, Phys. Rev. B **26**, 701 (1982).

[34] A. Le Bail, H. Duroy, and J. L. Fourquet, Mater. Res. Bull. **23**, 447 (1988).

[35] P. J. Brown, J. Crangle, T. Kanomata, M. Matsumoto, K.-U. Neumann, B. Ouladdiaf, and K. R. A. Ziebeck, J. Phys.: Condens. Matter **14**, 10159 (2002); J. Pons, R. Santamarta, V. A. Chernenko, and E. Cesari, J. Appl. Phys. **97**, 083516 (2005); R. Ranjan, S. Banik, U. Kumar, P. K. Mukhopadhyay, S. R. Barman, and D. Pandey, Phys. Rev. B **74**, 224443 (2006); L. Righi, F. Albertini, G. Calestani, L. Rareti, A. Paoluzi, C. Ritter, P. A. Algarabel, L. Morellon, and M. R. Ibarra, J. Solid State Chem. **179**, 3525 (2006).

[36] K. Bhattacharya, *Microstructure of Martensite. Why It Forms and How It Gives Rise to the Shape-Memory Effect* (Oxford University Press, Oxford, 2003).

[37] F. Albertini, L. Pareti, A. Paoluzi, L. Morellon, P. A. Algarabel, M. R. Ibarra, and L. Righi, Appl. Phys. Lett. **81**, 4032 (2002).

[38] P. J. Webster, K. R. A. Ziebeck, S. L. Town, and M. S. Peak, Philos. Mag. B **49**, 295 (1984).

[39] D. Hobbs, J. Hafner, and D. Spisak, Phys. Rev. B **68**, 014407

(2003).
[40] O. I. Velikokhatnyi and I. I. Nuamov, Phys. Solid State **41**, 617 (1999).
[41] E. Bauer, St. Berger, A. Galatanu, M. Galli, H. Michor, G. Hilscher, Ch. Paul, B. Ni, M. M. Abd-Elmeguid, V. H. Tran, A. Grytsiv, and P. Rogl, Phys. Rev. B **63**, 224414 (2001).
[42] S. von Molnar, R. J. Gambino, and J. M. D. Ceoy, J. Appl. Phys. **52**, 2193 (1981); A. Fert and R. Asomoza, *ibid.* **50**, 1886 (1979).
[43] E. V. Sampathkumaran and I. Das, Phys. Rev. B **51**, 8631 (1995); C. Mazumdar, A. K. Nigam, R. Nagarajan, C. Godart, L. C. Gupta, B. D. Padalia, G. Chandra, and R. Vijayaraghavan, Appl. Phys. Lett. **68**, 3647 (1996); A. K. Nigam, S. B. Roy, and P. Chaddah, Phys. Rev. B **60**, 3002 (1999); S. Radha, S. B. Roy, and A. K. Nigam, J. Appl. Phys. **87**, 6803 (2000).
[44] A. Gerber, I. Kishon, I. Ya. Korenblit, O. Riss, A. Segal, M. Karpovski, and B. Raquet, Phys. Rev. Lett. **99**, 027201 (2007).
[45] M. Shatzkes, P. Chaudhari, A. A. Levi, and A. F. Mayadas, Phys. Rev. B **7**, 5058 (1973).
[46] X. Jin, D. Bono, C. Henry, J. Feuchtwanger, S. M. Allen, and R. C. O'Handley, Philos. Mag. **83**, 3193 (2003).
[47] K. S. Sokhey, M. Manekar, M. K. Chattopadhyay, R. Kaul, S. B. Roy, and P. Chaddah, J. Phys. D **36**, 1366 (2003).
[48] C. Biswas, S. Banik, A. K. Shukla, R. S. Dhaka, V. Ganesan, and S. R. Barman, Surf. Sci. **600**, 3749 (2006).
[49] J. F. Gregg, W. Allen, K. Ounadjela, M. Viret, M. Hehn, S. M. Thompson, and J. M. D. Coey, Phys. Rev. Lett. **77**, 1580 (1996).
[50] D. Ravelosona, A. Cebollada, F. Briones, C. Diaz-Paniagua, M. A. Hidalgo, and F. Batallan, Phys. Rev. B **59**, 4322 (1999).
[51] W. Gil, D. Görlitz, M. Horisberger, and J. Kötzler, Phys. Rev. B **72**, 134401 (2005).
[52] K. M. Seemann, V. Baltz, M. MacKenzie, J. N. Chapman, B. J. Hickey, and C. H. Marrows, Phys. Rev. B **76**, 174435 (2007).
[53] J. Marcos, A. Planes, L. Mañosa, F. Casanova, X. Batlle, A. Labarta, and B. Martínez, Phys. Rev. B **66**, 224413 (2002).
[54] A. A. Likhachev, A. Sozinov, and K. Ullakko, Mater. Sci. Eng., A **378**, 513 (2004).
[55] S. Jeong, K. Inoue, S. Inoue, K. Koterazawa, M. Taya, and K. Inoue, Mater. Sci. Eng., A **359**, 253 (2003).
[56] M. Pasquale, C. Sasso, S. Besseghini, F. Passaretti, E. Villa, and A. Sciacca, IEEE Trans. Magn. **36**, 3263 (2000).
[57] U. Gaitzsch, M. Potschke, S. Roth, B. Rellinghaus, and L. Schultz, Scr. Mater. **57**, 493 (2007).
[58] H. D. Chopra and C. Ji, Phys. Rev. B **61**, R14913 (2000).
[59] O. Söderberg, Y. Ge, N. Glavatska, O. Heczko, K. Ullakko, and V. K. Lindroos, J. Phys. IV **11**, Pr8-287 (2001); S. Guo, Y. Zhang, B. Quan, J. Li, and X. Wang, Mater. Sci. Forum **475-479**, 2009 (2005).